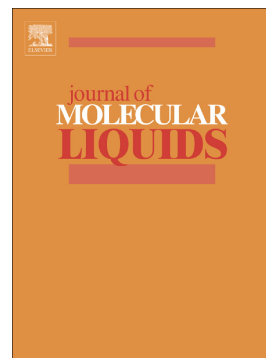


Journal Pre-proof

A new aggregation-induced emission active red-emitting fluorescent sensor for ultrarapidly, selectively and sensitively detecting hydrazine and its multiple applications

Pengcheng Yin, Qingfen Niu, Tianduo Li, Tao Wei, Jianbin Chen, Xuyang Qin



PII: S0167-7322(20)33528-5

DOI: <https://doi.org/10.1016/j.molliq.2020.113845>

Reference: MOLLIQ 113845

To appear in: *Journal of Molecular Liquids*

Received date: 2 June 2020

Revised date: 10 July 2020

Accepted date: 14 July 2020

Please cite this article as: P. Yin, Q. Niu, T. Li, et al., A new aggregation-induced emission active red-emitting fluorescent sensor for ultrarapidly, selectively and sensitively detecting hydrazine and its multiple applications, *Journal of Molecular Liquids* (2020), <https://doi.org/10.1016/j.molliq.2020.113845>

This is a PDF file of an article that has undergone enhancements after acceptance, such as the addition of a cover page and metadata, and formatting for readability, but it is not yet the definitive version of record. This version will undergo additional copyediting, typesetting and review before it is published in its final form, but we are providing this version to give early visibility of the article. Please note that, during the production process, errors may be discovered which could affect the content, and all legal disclaimers that apply to the journal pertain.

A new aggregation-induced emission active red-emitting fluorescent sensor for ultrarapidly, selectively and sensitively detecting hydrazine and its multiple applications

Pengcheng Yin, Qingfen Niu*, Tianduo Li, Tao Wei, Jianbin Chen, Xuyang Qin

Shandong Provincial Key Laboratory of Molecular Engineering, School of Chemistry and Pharmaceutical Engineering, Qilu University of Technology (*Shandong Academy of Sciences*), Jinan 250353, People's Republic of China

ABSTRACT

In this work, a novel carbazole-indandione based red-emitting fluorescent sensor **CBI** was developed, which exhibited typical and interesting aggregation-induced emission (AIE) characteristics with a large Stokes shift in mixed aqueous media. **CBI** as a colorimetric and fluorimetric sensor for sensing hydrazine in $\sim 100\%$ aqueous media shows ultrarapid response, excellent selectivity, and great sensitivity with a low detection limit of 1.18 ppb. The mechanism of **CBI** for highly sensing hydrazine was proved by fluorescence, FTIR, ^1H NMR and HRMS spectra. Interestingly, the **CBI** was not only applied to sensitively detect aqueous N_2H_4 in water, human urine and live cells, but also was conveniently utilized to visualize gaseous N_2H_4 with sensitive naked-eye color diversification. Additionally, owing to its intense fluorescence irradiated by UV light, the **CBI** was significantly used as a new fluorescent ink for writing and drawing as well as a writable fluorescent display material.

Keywords: Aggregation-induced emission; Fluorescent sensor; Red-emitting; Hydrazine detection; Bio-imaging; Fluorescent ink.

* To whom the correspondence should be addressed

E-mail: qf_niu1216@qlu.edu.cn

Telephone: +86(531)89631760

Fax number: +86(531)89631208

1. Introduction

Hydrazine (N_2H_4), not only was widely used for the manufacture of dyes, photosensitizers, pharmaceuticals, emulsifiers and pesticides because of its strong reducing properties [1–3], but also applied as a high-energy fuel in rocket propulsion system due to its explosive characteristics [4–6]. Additionally, ascribing to its excellent water solubility and high toxicity, hydrazine is easy to cause environmental pollution and serious damage to the human health [7,8]. The U.S. Environmental Protection Agency (USEPA) has set the threshold limit of hydrazine is 10 ppb [9]. Hence, it is urgently demanded to develop an effective, convenient and reliable method for sensitively determining hydrazine in enviro/biological systems.

In recent years, several methods have been reported for detecting hydrazine, such as high-performance liquid chromatography (HPLC) [10], coulometry [11], and electrochemistry [12]. Fluorescent sensors are more attractive and advantageous over other conventional methods for biological and environmental cations and anions as well as active molecules in terms of their rapidity, reliability, simplicity and significant potential for bioimaging [13–33]. Up to now, numerous fluorescent sensors for N_2H_4 detection have been developed [34–40]. However, some fluorescent sensors still has some shortcomings such as sluggish response, poor selectivity and inferior sensitivity, which suffer from their practical

applications. Thus, the exploitation of novel fluorescent sensors for N_2H_4 detection with outstanding features and multiple practical applications, which could effectively overcome the existent shortcomings, are still highly demanded.

Luminogens of aggregation-induced emission (AIE) have attracted tremendous attention as that they are poor emission in solution but show highly emissive upon aggregation [41]. Because of the interesting fluorescence characteristics and great application potentials, AIE-active luminogens have been extensively developed and applied as chemo/biosensors and smart materials [42–44]. Recently, great efforts have been devoted to the extensively developing new AIE-active fluorescent sensors for sensitive and quantitative recognition of various environmental and biological analytes since they display a remarkable advantage of high adaptability to working conditions [41,456–47]. Unfortunately, most of the reported AIE-active fluorescent sensors dominantly emit green/blue fluorescence [48–50], while quite few are red-emitting. Hence, developing new AIE-active red-emitting fluorescent sensors are highly desirable.

Herein, we report a new carbazole-indandione based AIE active red-emitting fluorescent sensor **CBI**, and was utilized for sensitive, specific, colorimetric and fluorimetric detection of N_2H_4 in $\sim 100\%$ aqueous solution. Interestingly, **CBI** exhibits good features of

red-emitting fluorescence, large Stokes shift (170 nm), ultrarapid fluorescence response (50 s), low cytotoxicity (cell viability > 90%) and outstanding biocompatibility. In addition, **CBI** displays a highly selective fluorescence quenching effect toward N_2H_4 with low detection limit of 1.18 ppb. Interestingly, sensor **CBI** can be utilized as a new fluorescent ink and a writable molecular smart fluorescent display material. More importantly, the **CBI** is applied to monitor and image aqueous N_2H_4 in real water, human urine, live cells, as well as visualize gaseous hydrazine.

2. Experimental part

2.1. Reagents and instruments

All chemicals (including active small molecules: N_2H_4 , Cys, Hcy, GSH, urea, thiourea, NH_2OH , EDA, Ph- NH_2 , TEA, NH_3 , n-Bu NH_2 , various anions including F^- , Br^- , Cl^- , CN^- and AcO^- obtained from their tetrabutylammonium or sodium salts, and various cations including Na^+ , Al^{3+} , Cr^{3+} , Cd^{2+} , Co^{2+} , Mg^{2+} , Hg^{2+} and Fe^{2+} obtained from their nitrate salts) were purchased from Alfa Aesar Co. (Tianjin, China), which were of analytical grade and were used without further purification. 1H and ^{13}C nuclear magnetic resonance (NMR) spectra were recorded on a Bruker 400 MHz spectrophotometer using $DMSO-d_6$ and tetramethylsilane (TMS) as a solvent and an internal standard, respectively. High-resolution mass spectra (HRMS) were obtained using a Q-TOF6510 spectrograph (Agilent). Infrared spectra (IR) were performed using a Shimadzu

FTIR-8100 spectrophotometer. Optical absorption spectra were measured using a Shimadzu UV-2600 spectropolarimeter at room temperature. Fluorescence spectra were recorded using an Edinburgh Ltd-FLS920 spectrofluorophotometer. For all fluorescent measurements, both excitation and emission slit widths were 5 nm. The pH was tested on a Model PHS-25 pH meter. The bioimaging was tested using a Leica TCS SP8 confocal-laser scanning microscope (CLSM) ($\lambda_{\text{ex}} = 552 \text{ nm}$).

2.2. General spectroscopic procedures

Sensor **CBI** was dissolved in EtOH to prepare the stock solution of $1 \times 10^{-3} \text{ M}$. The other various testing species, including primary amines such as N_2H_4 , Cys, Hcy, GSH, urea, thiourea, NH_2OH , EDA, Ph- NH_2 , TEA, NH_3 , n-Bu NH_2 , representative cations (Na^+ , Al^{3+} , Cr^{3+} , Cd^{2+} , Co^{2+} , Mg^{2+} , Hg^{2+} , Fe^{2+}) and representative anions (CN^- , CH_3COO^- , F^- , Br^- , Cl^-) were subsequently dissolved in deionized water to provide the stock solutions ($1 \times 10^{-3} \text{ M}$). The analytical solutions were prepared by diluting reserve solution with the deionized water, and then shaken well and kept for 0.5 h before taking the optical spectra. All spectral tests were performed in $\sim 100\%$ aqueous solution at room temperature ($\lambda_{\text{ex}} = 445 \text{ nm}$).

2.3. Fluorescence quantum yield

The relative fluorescence quantum yield (Φ) was evaluated by quinine sulfate as reference and calculated by the following formula:

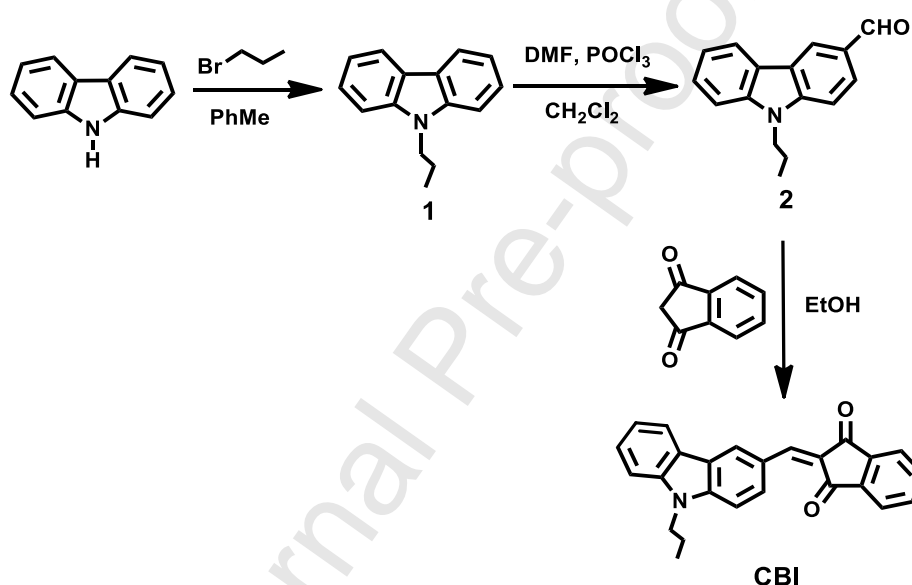
$$\Phi_s = \Phi_r (A_r/A_s)(I_s/I_r)(\eta_s^2/\eta_r^2)$$

Where Φ_s and Φ_r represent the quantum yield of sample and the quinine sulfate ($\Phi = 0.55$, 0.1 N H₂SO₄), A_r and A_s represent the absorbance of reference and sample, I_s and I_r represent the integrated fluorescence intensity of sample and reference, and η represents the refractive index of the solvent, respectively.

2.4. Synthesis of 2-((9-propyl-9H-carbazol-3-yl)methylene)-1H-indene-1,3(2H)-dione (**CBI**)

N-propylcarbazole (**1**) and N-propylcarbazole-3-carbaldehyde (**2**) were prepared as the previously reported procedure [51,52]. The **Scheme 1** clearly showed that the **CBI** was synthesized by the Knoevenagel condensation reaction between N-propylcarbazole-3-carbaldehyde and indandione. Compound **2** (80 mg, 0.34 mmol), indandione (50 mg, 0.34 mmol) and dry ethanol (10 mL) were heated to reflux for 5 h. Then this reaction system was cooled to room temperature, and the final product was collected by the recrystallization to give compound **CBI** as an orange solid (95 mg, 76.6% yield). ¹H NMR (400 MHz, DMSO-d₆, ppm): δ = 9.51 (s, 1H), 8.78 (d, J = 8.0 Hz, 1H), 8.16 (d, J = 8.0 Hz, 1H), 7.97 (s, 1H), 7.82-7.93 (m, 4H), 7.76 (d, J = 8.0 Hz, 1H), 7.66 (d, J = 8.0 Hz, 1H), 7.47 (t, J = 8.0 Hz, 1H), 7.27 (t, J = 8.0 Hz, 1H), 4.38 (t, J = 8.0 Hz, 2H), 1.72-1.81 (m, 2H), 0.81 (t, J = 8.0 Hz, 3H); ¹³C NMR (100 Hz, DMSO-d₆, ppm): δ = 197.4, 190.6, 189.6, 148.2, 143.9, 142.2, 141.3, 139.7, 136.0,

135.9, 133.1, 129.2, 127.3, 125.7, 124.8, 123.3, 123.2, 123.1, 122.8, 121.0, 110.9, 110.4, 44.6, 22.4, 11.8; FTIR (KBr, cm^{-1}): $\nu = 1560$ (C=C), 1670 (C=O); HRMS (ESI): m/z $[\text{M}+\text{H}]^+$ calcd. for: $\text{C}_{25}\text{H}_{19}\text{NO}_2$: 366.1416, found: 366.1494. The structure of **CBI** was confirmed by the spectra of ^1H NMR, ^{13}C NMR, FTIR and HRMS (**Figs. S1–S4**), demonstrating the **CBI** was successfully prepared.



Scheme 1 The preparation of sensor **CBI**.

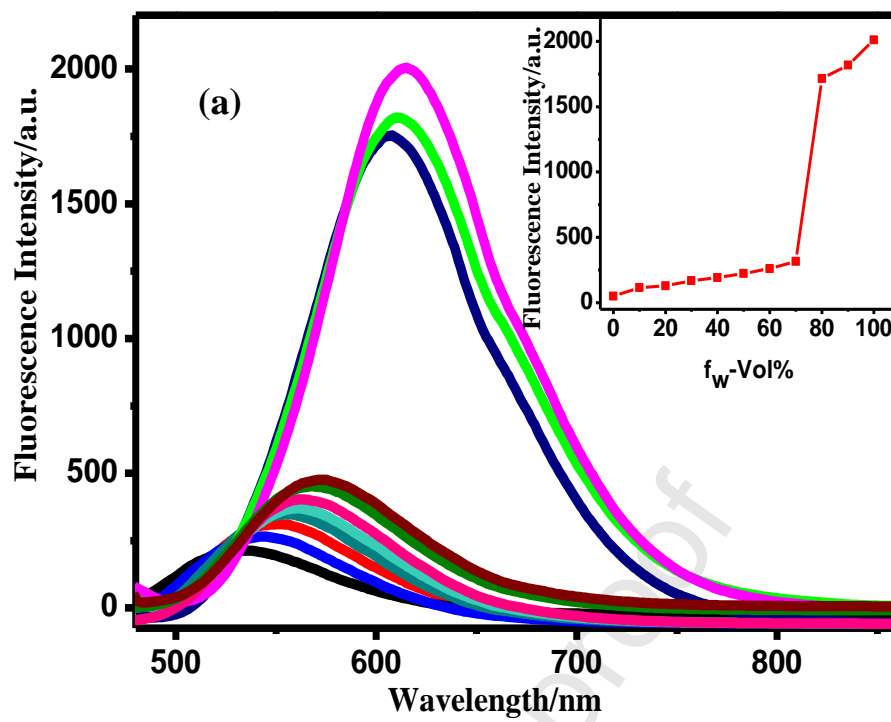
2.5. Bioimaging of living cells

The $20\ \mu\text{M}$ **CBI** was firstly incubated in HeLa cells within culture media for 0.5 h at 37°C , then washed 3 times using PBS. The cells were further treated with $20\ \mu\text{M}$ N_2H_4 in cell media for 0.5 h, then washed the media using PBS. The CLSM cell imaging was collected under the red channel (600-650 nm).

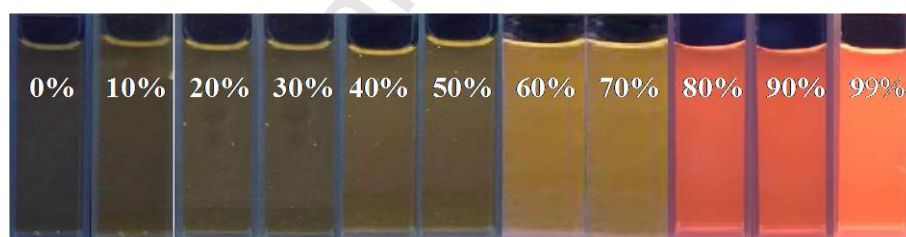
3. Results and discussion

3.1. AIE property of **CBI**

To explore the AIE property of **CBI**, the emission spectra in EtOH/H₂O (0~99%, v/v) solution were investigated. **CBI** is highly soluble in EtOH, but it is hardly to dissolve in water. As shown in **Fig. 1**, when the H₂O content was < 80%, the **CBI** (10 μM) was non-emissive ($\lambda_{\text{ex}} = 445 \text{ nm}$). However, a distinct broad emission at 615 nm was observed and red-shifted greatly (80 nm) when the H₂O fraction exceeded 80%, and then reached the strongest emission intensity at $f_w = 99\%$, with the relative emission intensity (I/I_0) at 615 nm up to 44-fold (**Fig. 1a, inset**), implying the typical AIE activity of **CBI** in aqueous media. Moreover, the AIE feature of **CBI** can be directly observed by the fluorescence color change from colorless to red when increasing the proportion of water in the EtOH/H₂O mixture (**Fig. 1b**). The fluorescence quantum yields (Φ) of **CBI** in EtOH and EtOH/H₂O ($f_w = 99\%$) were determined to be 1.04% and 39.1%, respectively, using quinine sulfate ($\Phi = 0.55$) as standard [53]. In addition, the typical AIE characteristics were also confirmed by its solid luminescence. As displayed in **Fig. 1c**, the **CBI** exhibits an intense fluorescence emission at 609 nm with a large Stokes shift (164 nm) in the solid state, and emits intense yellow fluorescence ($\Phi = 0.37$) under UV light. These findings revealed that **CBI** is a typical AIE-active compound.



(b)



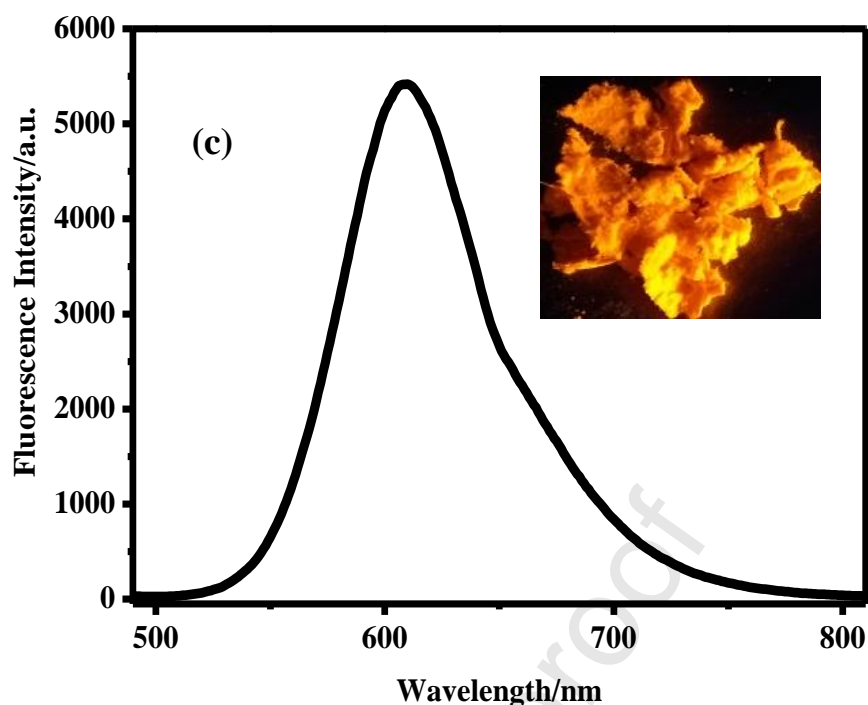


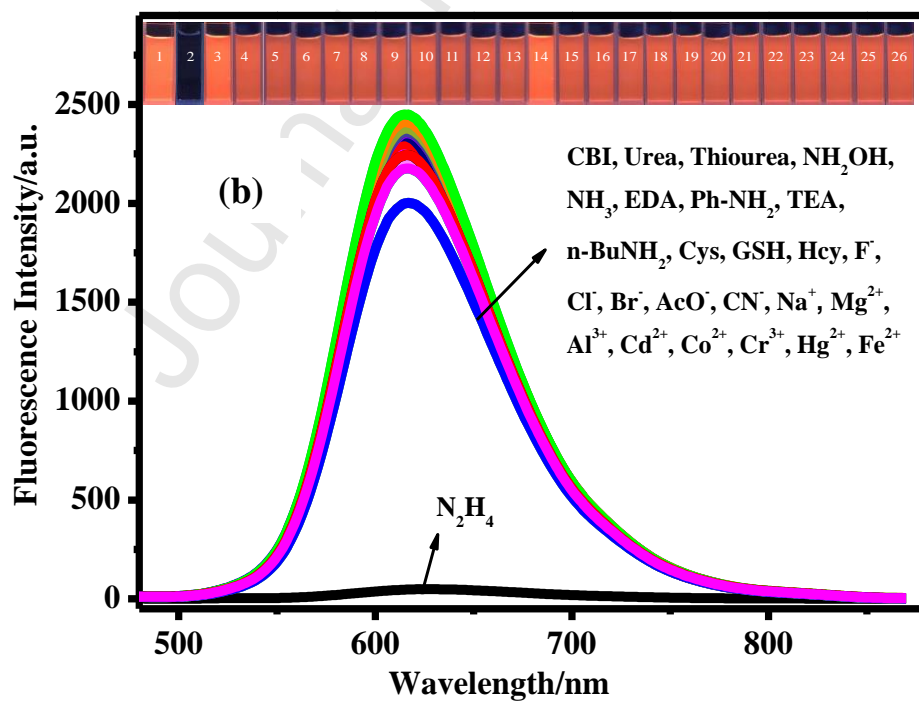
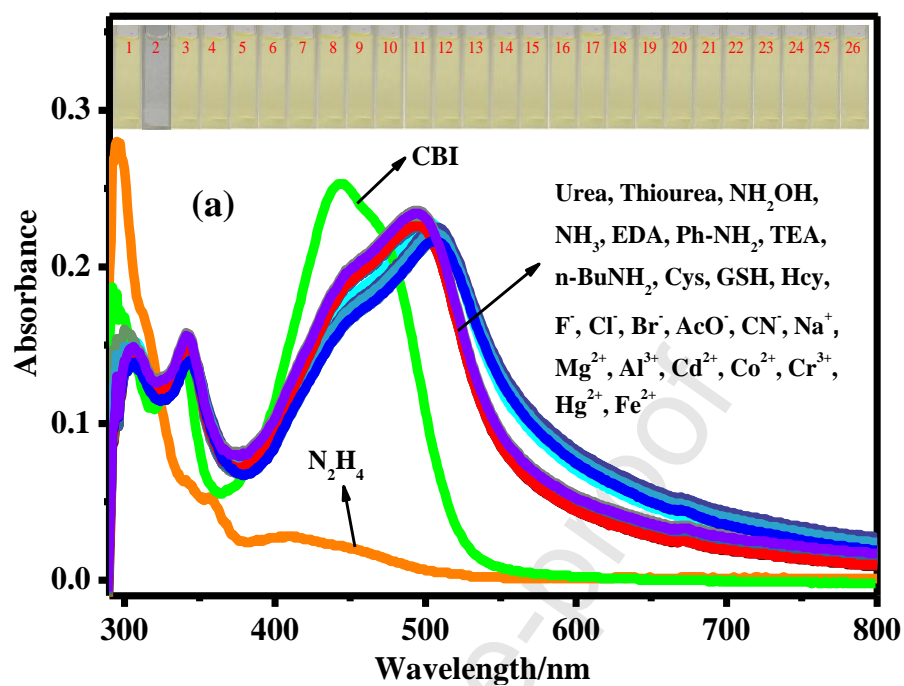
Fig. 1 (a) Fluorescence emission spectra of 10 μM sensor **CBI** in different EtOH/H₂O (v/v) mixtures; (b) Photographs of **CBI** in EtOH/H₂O mixtures with various H₂O fractions (f_w 0~99%) taken under 365 nm UV illumination; (c) The fluorescence emission spectrum of the **CBI** in solid state; **Inset:** Image of **CBI** in solid state under UV light.

3.2. Optical response to hydrazine

The optical behavior of chemosensor **CBI** toward hydrazine in \sim 100% aqueous media were investigated by the absorption and emission method. As shown in **Fig. 2a**, the absorption spectrum of **CBI** (10 μM) shows two distinct bands at 339 and 445 nm corresponding to the π - π^* and intramolecular charge transfer (ICT) transitions, respectively, and its solution color was pale yellow. The adding 2.0 equiv. of hydrazine to the sensor **CBI** solution, the bands decreases drastically in absorption along

with its solution color distinctly changed to colorless, which enables it to distinguish N_2H_4 by the naked eye. Whereas, the adding 2.0 equiv. of with other various relevant analytes (Cys, Hcy, GSH, urea, thiourea, NH_2OH , EDA, Ph- NH_2 , TEA, NH_3 , n-Bu NH_2 , Na^+ , Al^{3+} , Cr^{3+} , Cd^{2+} , Co^{2+} , Mg^{2+} , Hg^{2+} , Fe^{2+} , CN^- , F^- , Br^- , Cl^- and AcO^-) to **CBI** solution only led to a slight red shifted band at *ca.* 494 nm, no noticeable visual color was found, which is due to the solid precipitation in the solution. As shown in **Fig. 2b**, the fluorescence spectrum of **CBI** (10 μM) exhibits a strong red emission at 615 nm when excited at 445 nm. The addition of various analytes (2.0 equiv.) to **CBI** solution, only N_2H_4 induced a drastic fluorescence quenching behavior, along with a distinct fluorescence color change from red to colorless by the naked eyes, and no noticeable fluorescence variation was observed by adding other analytes. These investigations suggested the high selectivity of the **CBI** for N_2H_4 . The high specificity of **CBI** towards N_2H_4 was proved by the competitive experiments. The **CBI** was treated with 20 μM N_2H_4 in the presence of 20 μM other potential interfering species such as Cys, Hcy, GSH, urea, thiourea, NH_2OH , EDA, Ph- NH_2 , TEA, NH_3 , n-Bu NH_2 , Na^+ , Al^{3+} , Cr^{3+} , Cd^{2+} , Co^{2+} , Mg^{2+} , Hg^{2+} , CN^- , F^- , Br^- , Cl^- and AcO^- . The **Fig. 2c** shows a great fluorescence quenching when **CBI** treated with N_2H_4 , which was hardly disturbed by other tested interfering species, demonstrating that sensor **CBI** for N_2H_4 had excellent selectivity over a variety of interfering

species.



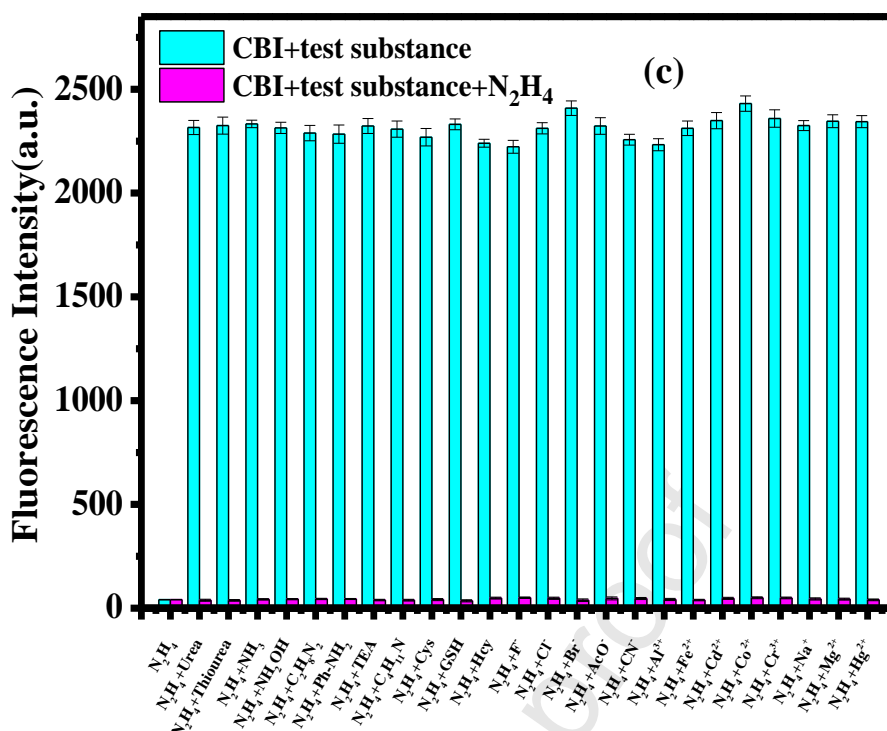
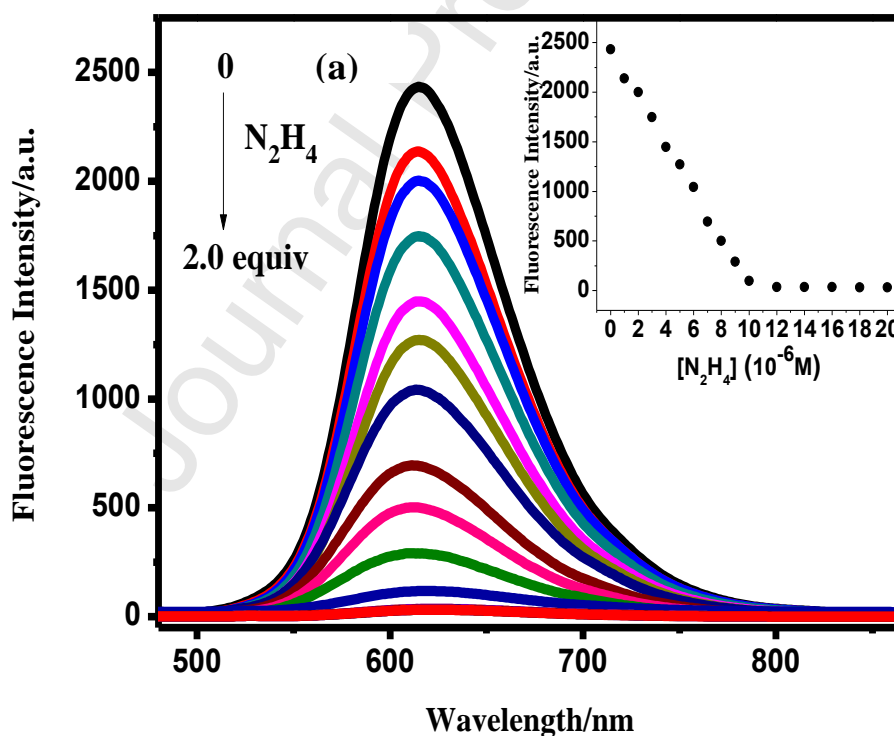


Fig. 2 Absorption (a) and fluorescence emission (b) spectra of the **CBI** (10 μ M) when adding different test substances (2.0 equiv.); **Insets:** Colorimetric and fluorimetric responses of **CBI** (10 μ M) towards various test substances (2.0 equiv.) (1-26: free **CBI**, N₂H₄, urea, thiourea, NH₂OH, NH₃, EDA, Ph-NH₂, TEA, n-BuNH₂, Cys, GSH, Hcy, F⁻, Cl⁻, Br⁻, AcO⁻, CN⁻, Na⁺, Mg²⁺, Al³⁺, Cd²⁺, Co²⁺, Cr³⁺, Hg²⁺, Fe²⁺); (c) Competitive experiments of **CBI** (10 μ M) at 615 nm toward N₂H₄ (2.0 equiv.) over various test substances (2.0 equiv.).

To evaluate the sensitivity of **CBI** towards hydrazine, the fluorescence titration of **CBI** treated with different amounts of hydrazine (0-2.0 equiv.) was conducted. As illustrated in **Fig. 3a**, the emission at 615 nm gradually decreased with the increasing hydrazine and peaked

when added 10 μM hydrazine. **Fig. 3b** demonstrated that fluorescence intensity at 615 nm of **CBI** varying with the hydrazine concentration showed good linearity ($R^2 = 0.99691$) in the range of 0–10 μM , accompanied with a prominent change in solution color. Moreover, according to the $DL = 3\sigma/k$ [54], the low detection limit of **CBI** was calculated to be 37 nM (1.18 ppb). This DL value is not only quite lower than the USEPA threshold concentration of 10 ppb [9], but only is comparable with some reported sensors (**Table S1**), demonstrating that **CBI** was indeed a sensitive sensor for quantitatively detecting hydrazine.



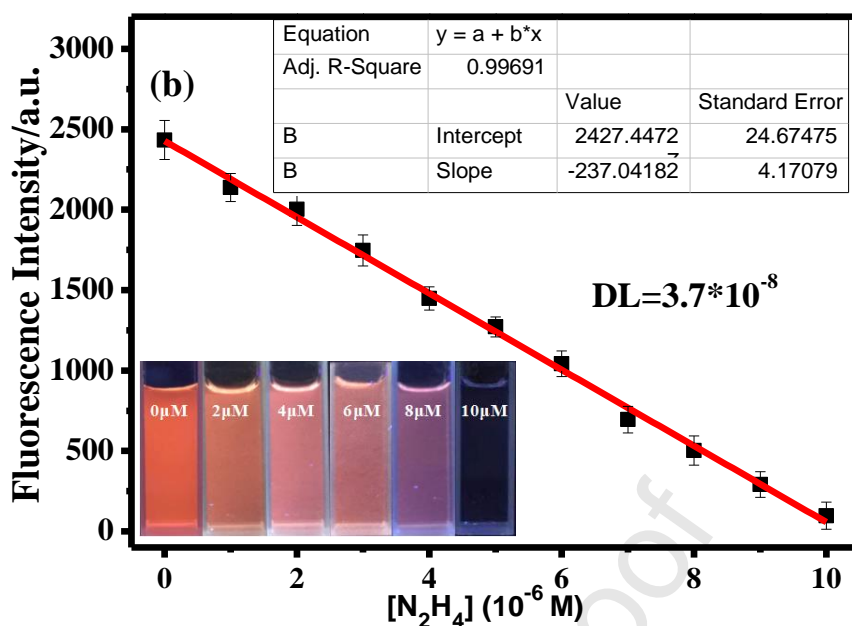


Fig. 3 (a) Fluorescence emission spectra of **CBI** (10 μ M) upon addition of N_2H_4 (0–2.0 equiv.) in \sim 100% aqueous solution; **Inset:** Plot of fluorescence emission intensity (615 nm) of **CBI** versus $[N_2H_4]$. **(b)** Fluorescence emission intensity (615 nm) changes of the **CBI** with gradual addition of N_2H_4 (0–10 μ M); **Inset:** Photographs of **CBI** treated with various N_2H_4 concentrations.

The time-dependent fluorescent response of **CBI** with 2.0 equivalent of hydrazine was studied (**Fig. S5**). It was clearly found that the emission intensity at 615 nm decreased immediately and achieved a stable state at 50 s, indicating that the reaction is complete within 50 s, and the **CBI** was quite useful for ultrarapidly detecting hydrazine.

The recognition behavior of the **CBI** for hydrazine at varied pH was also studied (**Fig. S6**). When the pH value was varied from 1.0 to 12.0,

free **CBI** solution showed negligible fluorescence signal change, indicating that **CBI** is pH-uninfluenced and high stable in a wide pH range. However, when 2.0 equiv. hydrazine was added, the fluorescence intensity of the **CBI** at 615 nm sharply decreased and kept stable in the pH range of 5.0–10.0, which was ascribed to the nucleophilicity of hydrazine under alkaline condition. Whereas, under the acidic conditions ($\text{pH} < 4$), the fluorescence intensity had no apparent change due to the protonation of hydrazine at low pH value, and weaken the nucleophilicity of hydrazine [55]. It is indicated that **CBI** can selectively detect N_2H_4 in a wide pH range of 5.0–10.0 including physiological conditions.

3.3. Response mechanism studies

To further confirm the interaction mechanism of **CBI** with N_2H_4 , the reaction of **CBI** with N_2H_4 was conducted. The product of **CBI** reacted with N_2H_4 was subjected to ^1H NMR, FTIR and HRMS spectral analysis. The ^1H NMR of **CBI** in DMSO-d_6 with/without hydrazine was firstly examined. As observed from **Fig. 4**, after the **CBI** being treated with hydrazine (1.0 equiv.), the characteristic proton signal for H_a (at 9.51 ppm) of **CBI** shifted to 8.09 ppm, which matched the characteristic chemical shift for H_a' of the byproduct. The aromatic proton signals (H_b at 8.78 ppm and H_c at 8.16 ppm) of **CBI** completely disappeared, and a proton signal H_d at 6.41 ppm ($\text{C}=\text{NNH}_2$) obviously appeared, indicating the decomposition of **CBI** by hydrazine and formation of a corresponding

hydrazone. The FTIR spectra of **CBI** before and after N_2H_4 provided another proof (**Fig. S7**). When treated with N_2H_4 , it was clearly observed that the characteristic stretching vibration absorption peak at 1670 cm^{-1} owing to carbonyl ($\text{C}=\text{O}$) group disappeared completely, together with a new absorption band emerged at 1625 cm^{-1} due to aldimine ($\text{C}=\text{N}$) group. Meanwhile, the appearance of new double absorption bands emerged at 3323 and 3394 cm^{-1} due to the hydrazone amine ($\text{C}=\text{N}-\text{NH}_2$) group. The reaction product of **CBI** and hydrazine was further identified by HRMS spectrum (**Fig. S8**). The HRMS spectrum showed a strong peak at $m/z = 252.1463$, which was identical to the corresponding adduct product **3** ($[\text{M}+\text{H}]^+ = 252.1422$). Additionally, the Job's plot analysis further proved the 1:1 stoichiometric reaction between **CBI** and N_2H_4 (**Fig. S9**). Based on the above facts, we concluded that the new species **3** was the obtained adduct product hydrazone by the **CBI** reacting with N_2H_4 , which blocked the ICT process and caused the fluorescence quenching because of the weaken withdrawing ability of the hydrazone amine group (**Scheme 2**). The proposed sensing mechanism was similar to that of the previously reported literature [56–61].

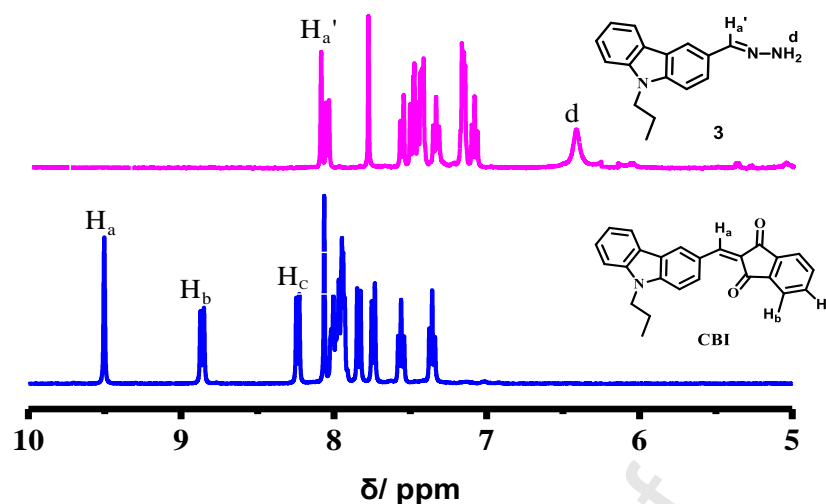
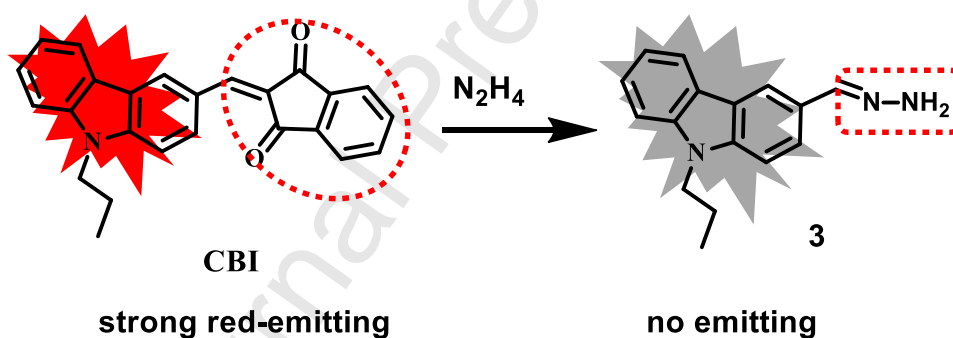


Fig. 4. ^1H NMR spectra before and after adding N_2H_4 to **CBI** (1.0 equiv) in DMSO-d_6 solution.



Scheme 2 The proposed mechanism of **CBI** for sensing N_2H_4 .

3.4. Application in water and urine samples

In terms of the excellent sensitivity of **CBI** for hydrazine sensing, the ability of the **CBI** to quantitatively detect hydrazine in distilled water, tap water, domestic water, Dacheng river water in Qilu University of Technology, the Yellow River water, and human urine samples was investigated applying a standard addition method. These crude samples

were firstly passed via a microfiltration membrane (0.22 μm), and then spiked with different hydrazine concentrations (2.5, 5 and 10 μM). As shown in **Table 1**, the tested results were consistent with the actual added amounts of hydrazine in each sample (recovery 98.2% \sim 101.3% with low RSD values). The spiked recoveries obtained were favorably compared with those reported recoveries (97.5% \sim 100.3%) using a standard method [62], indicating the feasibility of the sensor **CBI** for sensitively monitoring hydrazine in practical samples.

Table 1 Quantitative detection of N_2H_4 in real water and human urine samples.

Sample	Added (μM)	Detected ($\bar{x}\pm\text{SD}$) (μM)	Recovery (%)	RSD (%)	Standard error
Distilled water	2.5	2.51 \pm 0.026	100.4	1.05	0.027
	5	5.01 \pm 0.035	100.2	0.70	0.029
	10	10.04 \pm 0.135	100.4	1.34	0.110
Dacheng river water	2.5	2.49 \pm 0.020	99.6	0.80	0.016
	5	5.00 \pm 0.052	100	1.04	0.042
	10	9.93 \pm 0.072	99.3	0.73	0.059
Tap water	2.5	2.52 \pm 0.025	100.8	1.00	0.020
	5	4.99 \pm 0.025	99.8	0.51	0.021
	10	10.11 \pm 0.100	101.1	0.99	0.082
The Yellow river water	2.5	2.50 \pm 0.005	100	0.23	0.005
	5	4.98 \pm 0.035	99.6	0.71	0.029
	10	9.82 \pm 0.096	98.2	0.98	0.078
Domestic water	2.5	2.48 \pm 0.025	99.2	1.01	0.020
	5	4.97 \pm 0.007	99.4	1.41	0.057
	10	10.04 \pm 0.067	100.4	0.66	0.054
Human urine	2.5	2.47 \pm 0.006	98.8	0.23	0.005
	5	5.07 \pm 0.186	101.3	2.67	0.152
	10	10.00 \pm 0.038	99.6	0.38	0.031

3.4. Application as fluorescent ink

Taking the advantage of the strong fluorescence, the **CBI** could be used as a new type UV-activated fluorescent ink with a broad application prospect. The homogeneous aqueous solution of the **CBI** (10 μM) was injected into a vacant pen without any modification, which was directly used as fluorescent ink to write Chinese characters and patterns on the handwritten filter paper. As displayed in **Fig. 5**, all the Chinese characters and patterns emitted yellow fluorescence under UV light, which are highly distinct from the background. These results suggests that the **CBI** ink could be an alternative for traditional fluorescent pens.



Fig. 5. The photographic images of the Chinese characters and fluorescent patterns written on filter paper using aqueous **CBI** solution under a UV light.

3.5. Application as fluorescent display material

Considering its good fluorescent performance, the **CBI** could act as a writable molecular smart fluorescent display material. The **CBI** thin film was prepared by spreading out a **CBI** solution on the TLC plate. After being air-dried, a writing brush dipped in aqueous hydrazine (10 μ M) was used to write the chemical formula “ N_2H_4 ” on the film. Interestingly, under irradiation with 365 nm UV lamp, the bright yellow fluorescence was immediately changed to blue at a specific position by hydrazine exposure (**Fig. 6**). Thus, the simple **CBI** based thin-film could not only be utilized as a convenient hydrazine-sensitive solid fluorescent sensor but also as a writable fluorescent display material.

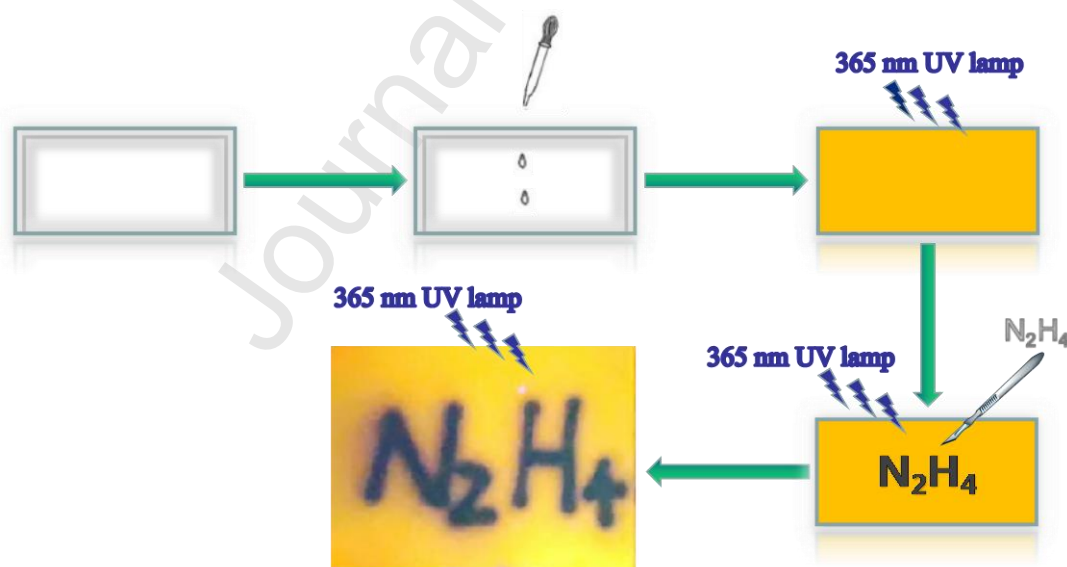


Fig. 6. The preparation and application of the sensor **CBI** based thin-film.

3.6. Visualization of gaseous hydrazine

Inspired by its excellent performance, the potential utility of **CBI** for sensitively visualize gaseous hydrazine was further evaluated. The filter-paper was firstly soaked in a stock solution of **CBI**. After air-dried, the **CBI**-loaded test strips were exposed to hydrazine vapor by being placed in sealed bottles containing different hydrazine concentrations (blank, 5%, 10%, 15%, 20%, 25%, w/w) for 10 min [63]. As shown in **Fig. 7**, as increasing the hydrazine concentration, distinctive color changes of the **CBI**-coated filter-papers were displayed from yellow to gray and the fluorescence color turn from bright yellow into white gray, which were highly dependent on the hydrazine concentration and easily distinguished by the naked eyes. These findings demonstrate that the **CBI**-loaded test strips approach is more convenient and instant visualization of gaseous hydrazine.

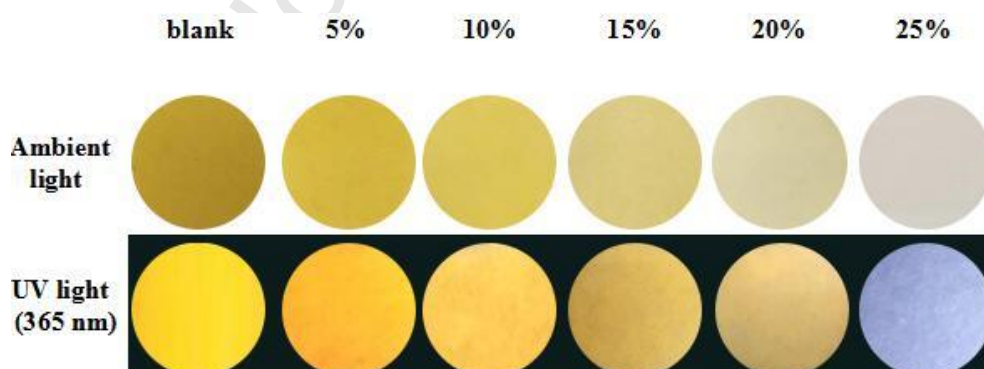


Fig. 7. The color variations of **CBI**-coated filter paper when exposed to hydrazine vapor for 10 min under ambient light and UV lamp (365 nm).

3.7. Bioimaging in live cells

The cytotoxicity of **CBI** was tested by a standard MTT assay toward HeLa cells. As illustrated in **Fig. 8a**, the cell viability is above 90% at the concentrations ranging from 0 to 30.0 μM for 24 hours. The results proved that the **CBI** has no marked cytotoxicity and suitable for bioimaging hydrazine in living cells. As displayed in **Fig. 8b**, after incubating the 25 μM **CBI** to HeLa cells for 30 min, the cells showed a remarkable red fluorescence, revealing **CBI** has good cell permeability. However, after the cells being treated with N_2H_4 (1.0 equiv) for 30 min, the red fluorescence was completely quenched, and almost no detectable fluorescence signal was found (**Fig. 8c**). This implied that the **CBI** was effectively attacked by N_2H_4 in live cells, and quenched drastically the fluorescence. These results demonstrate that **CBI** can be used for imaging N_2H_4 in cellular environment.

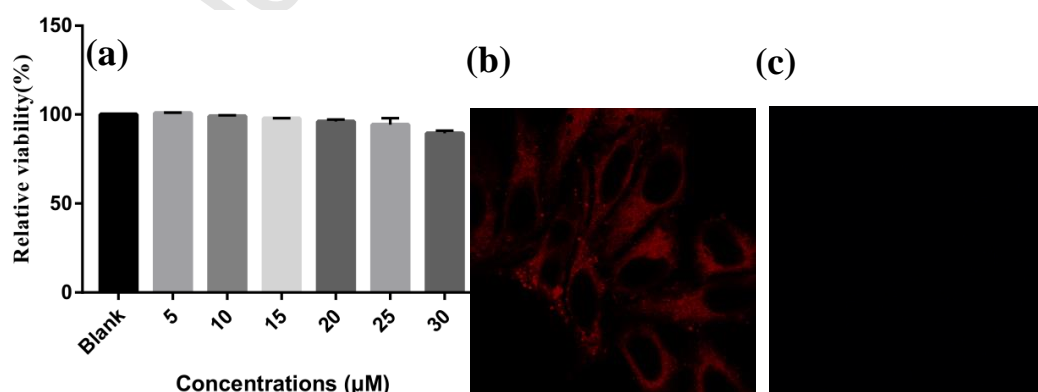


Fig. 8 (a) The cell viability of HeLa cells upon treatment of various

concentrations of **CBI**; Confocal fluorescence images of HeLa cells incubated with **CBI** before (**b**) and after (**c**) being treated with N_2H_4 for 0.5 h. Scale bar: 25 μm .

3.8. Comparison with other selective- N_2H_4 fluorescent sensors

Compared with some previously N_2H_4 -selective fluorescent sensors [59,64–67] (**Table S1**), our developed N_2H_4 -selective sensor **CBI** showed multitudinous attractive advantages of interesting AIE property, red-emitting with large Stokes shift, wide pH-range tolerance, ultrafast, colorimetric and fluorimetric responses, which was used for fluorescent ink, writable fluorescent display material, aqueous and gaseous detection, bioimaging, environmental and biological samples monitoring.

4. Conclusions

In summary, we reported a novel carbazole-indandione based red-emitting fluorescent sensor **CBI**, which displayed an interesting AIE active feature at a long wavelength of 615 nm and a large Stokes shift. Compared with presently N_2H_4 -selective fluorescent sensors, **CBI** shows ultrafast response, specific selectivity, great sensitivity and colorimetric/fluorimetric responses. The mechanism was confirmed by fluorescence, 1H NMR and HRMS spectra. Interestingly, the **CBI** thin film was prepared and displayed a remarkable luminescence response to hydrazine with great sensitivity, which can serve as a writable fluorescent display material. Besides, owing to its strong luminescence irradiated by

UV light, the **CBI** was significantly utilized as a new fluorescent ink for writing and drawing. Notably, the **CBI**-loaded test paper conveniently and sensitively detect gaseous hydrazine by color and fluorescence changes. Importantly, the **CBI** was used for sensitive detection of hydrazine in water, urine samples and cellular imaging, demonstrating its great potential in practical applications.

Acknowledgments

We greatly appreciate financial support from the National Natural Science Foundation of China (21801144, 21776143, 51702178), the Natural Science Foundation of Shandong Province (ZR2017LB009), the Ji Nan Science & Technology Bureau (2019GXRC021), the Youth Innovative Talents Recruitment and Cultivation Program of Shandong Higher Education, and the Program for Scientific Research Innovation Team in Colleges and Universities of Shandong Province.

References

- [1] H. Xu, B. Gu, Y. Li, Z. Huang, W. Su, X. Duan, P. Yin, H. Li, S. Yao, A highly selective, colorimetric and ratiometric fluorescent probe for NH_2NH_2 and its bioimaging, *Talanta* 180 (2018) 199–205.
- [2] J. Schalka, H. Oustadb, J.G. Kuenena, M.S.M. Jettena, The anaerobic oxidation of hydrazine: a novel reaction in microbial nitrogen metabolism, *FEMS Microbiol. Lett.* 158 (1998) 61–67.
- [3] Z. Li, W. Zhang, C. Liu, M. Yu, H. Zhang, L. Guo, L. Wei, A

- colorimetric and ratiometric fluorescent probe for hydrazine and its application in living cells with low dark toxicity, *Sens. Actuators B Chem.* 241 (2017) 665–671.
- [4] X. Yang, Y. Liu, Y. Wu, X. Ren, Z. Di, Y. Yong, A NIR ratiometric probe for hydrazine “naked eye” detection and its imaging in living cell, *Sens. Actuators B Chem.* 253 (2017) 488–494.
- [5] A.D. Sutton, A.K. Burrell, D.A. Dixon, E.B. Garner, J.C. Gordon, T. Nakagawa, K.C. Ott, J.P. Robinson, M. Vasiliu, Regeneration of ammonia borane spent fuel by direct reaction with hydrazine and liquid ammonia, *Science* 331 (2011) 1426–1429.
- [6] S.C. Jean, K. Asazawa, T.K. Sakamoto, K.J. Yamada, H. Tanaka, P. Strasser, Noble metal-Free hydrazine fuel cell catalysts: EPOC effect in competing chemical and electrochemical reaction pathways, *J. Am. Chem. Soc.* 133 (2011) 5425–5431.
- [7] S. Garrod, M.E. Bollard, A.W. Nicholls, S.C. Connor, J. Connelly, J. K. Nicholson, E. Holmes, Integrated metabonomic analysis of the multiorgan effects of hydrazine toxicity in the rat, *Chem. Res. Toxicol.* 18 (2005) 115–122.
- [8] International Agency for Research on Cancer: Re-evaluation of some organic chemicals, hydrazine, and hydrogen peroxide. IARC monographs on the evaluation of carcinogenic risk of chemicals to humans. Lyon, IARC; 1999, 71, 991.

- [9] O. o. R. a. D. a. U. S. Environmental Protection Agency (EPA), Integrated Risk Information System (IRIS) on hydrazine/hydrazine Sulfate, National Center for Environmental Assessment, DC, 1999.
- [10] P.E. Kester, N.D. Danielson, Determination of hydrazine and 1,1-dimethylhydrazine as salicyldehyde derivatives by liquid chromatography with electrochemical detection, *Chromatographia* 18 (1984) 125–128.
- [11] A.G. Fogg, A.Y. Chamsi, A.A. Barros, J.O. Cabral, Flow injection voltammetric determination of hypochlorite and hypobromite as bromine by injection into an acidic bromide eluent and the indirect determination of ammonia and hydrazine by reaction with an excess of hypobromite, *Analyst* 109 (1984) 901–904.
- [12] A. Umar, M.M. Rahman, S.H. Kim, Y.B. Hahn, Zinc oxide nanonail based chemical sensor for hydrazine detection, *Chem. Commun.* (2008) 166–168.
- [13] X. Chen, K.A. Lee, X. Ren, J.C. Ryu, G. Kim, J.H. Ryul, W.J. Lee, J. Yoon, Synthesis of a highly HOCl-selective fluorescent probe and its use for imaging HOCl in cells and organisms, *Nat. Protoc.* 11 (2016) 1219–1228.
- [14] C.X. Yin, K.M. Xiong, F.J. Huo, J.C. Salamanca, R.M. Strongin, Fluorescent Probes with Multiple Binding Sites for the Discrimination of Cys, Hcy, and GSH, *Angew. Chem. Int. Edit.* 56

- (2017) 13188–13198.
- [15] E.A. Specht, E. Braselmann, A.E. Palmer, A critical and comparative review of fluorescent tools for live-cell imaging, *Annu. Rev. Physiol.* 79 (2017) 93–117.
- [16] H.M. Lv, D.H. Yuan, W. Liu, Y. Chen, C.T. Au, S.F. Yin, A highly selective ESIPT-based fluorescent probe for cysteine sensing and its bioimaging application in living cells, *Sens. Actuators B Chem.* 233 (2016) 173–179.
- [17] P. Ghosh, J. Das, A. Basak, S.K. Mukhopadhyay, P. Banerjee, Nanomolar level detection of explosive and pollutant TNP by fluorescent aryl naphthalene sulfones: DFT study, in vitro detection and portable prototype fabrication, *Sens. Actuators B Chem.* 251 (2017) 985–992.
- [18] X. Wu, Q. Niu, T. Li, Y. Cui, S. Zhang, A highly sensitive, selective and turn-off fluorescent sensor based on phenylamine-oligothiophene derivative for rapid detection of Hg^{2+} , *J. Lumin.* 175 (2016) 182–186.
- [19] T. Sun, Q. Niu, Z. Guo, T. Li, A simple highly sensitive and selective turn-on fluorescent chemosensor for the recognition of Pb^{2+} , *Tetrahedron Lett.* 58 (2017) 252–256.
- [20] L. Lan, Q. Niu, T. Li, A highly selective colorimetric and ratiometric fluorescent probe for instantaneous sensing of Hg^{2+} in water, soil

- and seafood and its application on test strips, *Anal. Chim. Acta* 1023 (2018) 105–114.
- [21] J. Wang, T. Wei, F. Ma, T. Li, Q. Niu, A novel fluorescent and colorimetric dual-channel sensor for the fast, reversible and simultaneous detection of Fe^{3+} and Cu^{2+} based on terthiophene derivative with high sensitivity and selectivity, *J. Photoch. Photobio. A* 383 (2019) 111982.
- [22] Z. Guo, T. Hu, X. Wang, T. Sun, T. Li, Q. Niu, Highly sensitive and selective fluorescent sensor for visual detection of Cu^{2+} in water and food samples based on oligothiophene derivative, *J. Photoch. Photobio. A* 371 (2019) 50–58.
- [23] J. Wang, Q. Niu, T. Hu, T. Wei, T. Li, A new phenothiazine-based sensor for highly selective, ultrafast, ratiometric fluorescence and colorimetric sensing of Hg^{2+} : Applications to bioimaging in living cells and test strips, *J. Photoch. Photobio. A* 384 (2019) 112036.
- [24] Z. Zuo, X. Song, D. Guo, Z. Guo, Q. Niu, A dual responsive colorimetric/fluorescent turn-on sensor for highly selective, sensitive and fast detection of Fe^{3+} ions and its applications, *J. Photoch. Photobio. A* 382 (2019)111876.
- [25] Z. Guo, Q. Niu, T. Li, E. Wang, Highly chemoselective colorimetric/fluorometric dual-channel sensor with fast response and

- good reversibility for the selective and sensitive detection of Cu^{2+} , *Tetrahedron* 75 (2019) 3982–3992.
- [26] Z. Guo, Q. Niu, T. Li, T. Sun, H. Chi, A fast, highly selective and sensitive colorimetric and fluorescent sensor for Cu^{2+} and its application in real water and food samples, *Spectrochim. Acta A* 213 (2019) 97–103.
- [27] P. Yin, Q. Niu, Q. Yang, L. Lan, T. Li, A new “naked-eye” colorimetric and ratiometric fluorescent sensor for imaging Hg^{2+} in living cells, *Tetrahedron* 75 (2019) 130687.
- [28] P. Yin, Q. Niu, T. Wei, T. Li, Y. Li, Q. Yang, A new thiophene-based dual functional chemosensor for ultrasensitive colorimetric detection of Cu^{2+} in aqueous solution and highly selective fluorimetric detection of Al^{3+} in living cells, *J. Photoch. Photobio. A* 389 (2020) 112249.
- [29] C. Li, Q. Niu, J. Wang, T. Wei, T. Li, J. Chen, X. Qin, Q. Yang, Bithiophene-based fluorescent sensor for highly sensitive and ultrarapid detection of Hg^{2+} in water, seafood, urine and live cells, *Spectrochim. Acta A* 233 (2020) 118208.
- [30] C. Li, Q. Niu, T. Li, T. Wei, T. Hu, J. Chen, X. Qin, L. Yang, A novel dual-function bithiophene-Meldrum’s acid based chemosensor for highly sensitive, colorimetric and fluorimetric detection of

- cyanide and hypochlorite and its applications, *Dyes Pigm.* 180 (2020) 108459.
- [31] Z. Guo, Q. Niu, Q. Yang, T. Li, H. Chi, A highly selective and sensitive dual-mode sensor for colorimetric and turn-on fluorescent detection of cyanide in water, agro-products and living cells, *Anal. Chim. Acta* 1065 (2019) 113–123.
- [32] Z. Guo, T. Hu, T. Sun, T. Li, H. Chi, Q. Niu, A colorimetric and fluorometric oligothiophene-indenedione-based sensor for rapid and highly sensitive detection of cyanide in real samples and bioimaging in living cells, *Dyes Pigm.* 163 (2019) 667–674.
- [33] J. Wang, Q. Niu, T. Wei, T. Li, T. Hu, J. Chen, X. Qin, Q. Yang, L. Yang, Novel phenothiazine-based fast-responsive color/fluorimetric sensor for highly sensitive, selective and reversible detection of Cu^{2+} in real water samples and its application as an efficient solid-state sensor, *Microchem. J.* 157 (2020) 104990.
- [34] J.H. Zhu, H. Zhang, Y. Liao, J.J. Liu, Z.J. Quan, X.C. Wang, A multifunctional fluorescent probe for highly selective detection of hydrazine and discovering the interplay between AIE and ICT, *Dyes Pigm.* 175 (2020) 108111.
- [35] R.C. Gupta, S.K. Dwivedi, R. Ali, S.S. Razi, R. Tiwari, S. Krishnamoorthi, A. Misra, A sensitive TICT Probe exhibiting ratiometric fluorescence response to detect hydrazine in solution and

- gas phase, *Spectrochim. Acta A* 232 (2020) 118153.
- [36] X.C. Wang , G. Ding, Y.K. Duan, Y.J. Zhu, G.S. Zhu, M. Wang, X.J. Li, Y.F. Zhang, X.Z. Qin, C.H. Hung, A novel triphenylamine-based bis-Schiff bases fluorophores with AIE-Activity as the hydrazine fluorescence turn-off probes and cell imaging in live cells, *Talanta* 217 (2020) 121029.
- [37] X. Han, C. Tian, M.S. Yuan, Z.X. Li, W.J. Wang, T.B. Li, S.W. Chen, J.Y. Wang, Colorimetric hydrazine detection and fluorescent hydrogen peroxide imaging by using a multifunctional chemical probe, *Anal. Chim. Acta* 1052 (2019) 137–144.
- [38] J.T. Hou, B.Y. Wang, Y.Q. Wu, Y.X. Liao, W.X. Ren, Detection of hydrazine via a highly selective fluorescent probe: A case study on the reactivity of cyano-substituted C=C bond, *Dyes Pigm.* 178 (2020) 108366.
- [39] Z.D. Liu, Z.H. Yang, S.Z. Chen, Y. Liu, L.Q. Sheng, Z.M. Tian, D.Q. Huang, H. J. Xu, A smart reaction-based fluorescence probe for ratio detection of hydrazine and its application in living cells, *Microchem. J.* 156 (2020) 104809.
- [40] X.R. Shi, C.X. Yin, Y.B. Zhang, Y. Wen, F.J. Huo, A novel ratiometric and colorimetric fluorescent probe for hydrazine based on ring-opening reaction and its applications, *Sens. Actuators B Chem.* 285 (2019) 368–374.

- [41] J. Luo, Z. Xie, J.W. Lam, L. Cheng, H. Chen, C. Qiu, H.S. Kwok, X. Zhan, Y. Liu, D. Zhu, B.Z. Tang, Aggregation-induced emission of 1-methyl-1,2,3,4,5-pentaphenylsilole, *Chem. Commun.* 18 (2001) 1740–1741.
- [42] H.T. Feng, X. Zhang, Y.S. Zheng, Fluorescence Turn-on Enantioselective Recognition of both Chiral Acidic Compounds and α -Amino Acids by a Chiral Tetraphenylethylene Macrocyclic Amine, *J. Org. Chem.* 80 (2015) 8096–8101.
- [43] J.B. Xiong, W.Z. Xie, J.P. Sun, J.H. Wang, Z.H. Zhu, H.T. Feng, D. Guo, H. Zhang, Enantioselective Recognition for Many Different Kinds of Chiral Guests by One Chiral Receptor Based on Tetraphenylethylene Cyclohexylbisurea, *J. Org. Chem.* 81 (2016) 3720–3726.
- [44] J. Mei, N.L. Leung, R.T. Lwok, J.W. Lam, B.Z. Tang, Aggregation-Induced emission: together we shine, united we soar, *Chem. Rev.* 115 (2015) 11718–11940.
- [45] R. Hu, N.L.C. Leung, B.Z. Tang, AIE macromolecules: syntheses, structures and functionalities, *Chem. Soc. Rev.* 43 (2014) 4494–4562.
- [46] Y. Hong, J.W.Y. Lam, B.Z. Tang, Aggregation-induced emission: phenomenon, mechanism and applications, *Chem. Commun.* 29 (2009) 4332–4353.

- [47] Y. Hong, J.W.Y. Lam, B.Z. Tang, Aggregation-induced emission, *Chem. Soc. Rev.* 40 (2011) 5361–5388.
- [48] T. Han, Y. Hong, N. Xie, S. Chen, N. Zhao, E. Zhao, J.W.Y. Lam, H. H.Y. Sung, Y. Dong, B. Tong, B.Z. Tang, Defect-sensitive crystals based on diaminomaleonitrile-functionalized Schiff base with aggregation-enhanced emission, *J. Mater. Chem.* 1 (2013) 7314–7320.
- [49] T. Han, X. Gu, J.W.Y. Lam, A.C.S. Leung, R.T.K. Kwok, T. Han, B. Tong, J. Shi, Y. Dong, B.Z. Tang, Diaminomaleonitrile-based Schiff bases: aggregation-enhanced emission, red fluorescence, mechanochromism and bioimaging applications, *J. Mater. Chem.* 4 (2016) 10430–10434.
- [50] J. Gong, P. Wei, Y. Su, Y. Li, X. Feng, J.W.Y. Lam, D. Zhang, X. Song, B.Z. Tang, Red-emitting salicylaldehyde Schiff base with AIE behaviour and large Stokes shift, *Chin. Chem. Lett.* 29 (2018) 1493–1496.
- [51] C.B. Nielsen, T. Brock-Nannestad, P. Hammershøj, T.K. Reenberg, M. Schau-Magnussen, D. Trpceviski, T. Hensel, R. Salcedo, G.V. Baryshnikov, B.F. Minaev, M. Pittelkow, Azatrioxa circulenes: Planar Anti-Aromatic Cyclooctatetraenes, *Chem. Eur. J.* 19 (2013) 3898–904.
- [52] J. Luo, G.J. Song, X.J. Xing, S.L. Shen, Y.Q. Ge, X.Q. Cao, A simple

- but effective fluorescent probe for the detection of bisulfite, *New J. Chem.* 41 (2017) 3986–3990.
- [53] C. Wei, B.X. Sun, Z.L. Cai, Z.F. Zhao, Y. Tan, W.B. Yan, H.B. Wei, Z.W. Liu, Z.Q. Bian, C. Huang, Quantum yields over 80% achieved in luminescent europium complexes by employing diphenylphosphoryl tridentate ligands, *Inorg. Chem.* 57 (2018) 7512–7515.
- [54] H.M.N.H. Irving, H. Freiser, T.S. West, *IUPAC Compendium of Analytical Nomenclature, Definitive Rules*, Pergamon Press, Oxford, 1981.
- [55] J.T. Muckerman, J.H. Skone, M. Ning, Y.W. Tsutsui, Toward the accurate calculation of pKa values in water and acetonitrile, *BBA-Bioenergetics* 1827 (2013) 882–891.
- [56] Z.X. Li, W.Y. Zhang, C.X. Liu, M.M. Yu, H.Y. Zhang, L. Guo, L.H. Wei, A colorimetric and ratiometric fluorescent probe for hydrazine and its application in living cells with low dark toxicity, *Sens. Actuators B Chem.* 241 (2017) 665–671.
- [57] S.I. Reja, N. Gupta, V. Bhalla, D. Kaur, S. Arora, M. Kumar, A charge transfer based ratiometric fluorescent probe for detection of hydrazine in aqueous medium and living cells, *Sens. Actuators B Chem.* 222 (2016) 923–929.
- [58] M. Sun, J. Guo, Q. Yang, N. Xiao, Y. Li, A new fluorescent and

- colorimetric sensor for hydrazine and its application in biological systems, *J. Mater. Chem. B.* 2 (2014) 1846–1851.
- [59] Z. Chen, X.X. Zhong, W.B. Qu, T. Shi, H. Liu, H.P. He, X.H. Zhang, S.F. Wang, A highly selective HBT-based “turn-on” fluorescent probe for hydrazine detection and its application, *Tetrahedron Lett.* 58 (2017) 2596–2601.
- [60] Y. Liu, D. Ren, J. Zhang, H. Li, X.F. Yang, A fluorescent probe for hydrazine based on a newly developed 1-indanone-fused coumarin scaffold, *Dyes Pigm.* 162 (2019) 112–119.
- [61] Z. Guo, Q. Niu, Q. Yang, T. Li, T. Wei, L. Yang, J. Chen, X. Qin, New “naked-eye” colorimetric/fluorimetric “turn-on” chemosensor: Ultrafast and ultrasensitive detection of hydrazine in ~100% aqueous solution and its bio-imaging in living cells, *Anal. Chim. Acta* 1123 (2020) 64–72.
- [62] ASTM D1385–07 (2018)^{E1}, Standard Test Method for Hydrazine in Water, ASTM International, West Conshohocken, PA, 2018.
- [63] Q.Q. Wu, J.L. Zheng, W.C. Zhang, J.B. Wang, W.L. Liang, F.J. Stadler, A new quinoline-derived highly-sensitive fluorescent probe for the detection of hydrazine with excellent large-emission-shift ratiometric response, *Talanta* 195 (2019) 857–864.
- [64] S. Sinha, P. Gaur, S. Dev, S. Mukhopadhyay, T. Mukherjee, S. Ghosh, Hydrazine responsive molecular material: Optical signaling and

- mushroom cell staining, *Sens. Actuators B Chem.* 221 (2015) 418–426.
- [65] Y.Q. Song, G. Chen, X.Y. Han, J.M. You, F.B. Yu, A highly sensitive near-infrared ratiometric fluorescent probe for imaging of mitochondrial hydrazine in cells and in mice models, *Sens. Actuators B Chem.* 286 (2019) 69–76.*
- [66] H. Wang, Y.A. Li, S.X. Yang, H.Y. Tian, Y.G. Liu, B.G. Sun, A dual-function fluorescent probe for discriminative detection of hydrogen sulfide and hydrazine, *J. Photoch. Photobio. A.* 377 (2019) 36–42.
- [67] H. Wu, Y. Wang, W.N. Wu, Z.Q. Xu, Z.H. Xu, X.L. Zhao, Y.C. Fan, A novel ‘turn-on’ coumarin-based fluorescence probe with aggregation-induced emission (AIE) for sensitive detection of hydrazine and its imaging in living cells, *Spectrochim. Acta A* 222 (2019) 117272.

Author contributions

Pengcheng Yin: Conceptualization, Data curation, Software, Investigation, Writing-Original Draft.

Qingfen Niu: Resources, Writing-Review & Editing, Supervision, Data Curation.

Tianduo Li: Formal analysis, Review & Editing.

Tao Wei: Formal analysis, Review & Editing.

Jianbin Chen: Review & Editing.

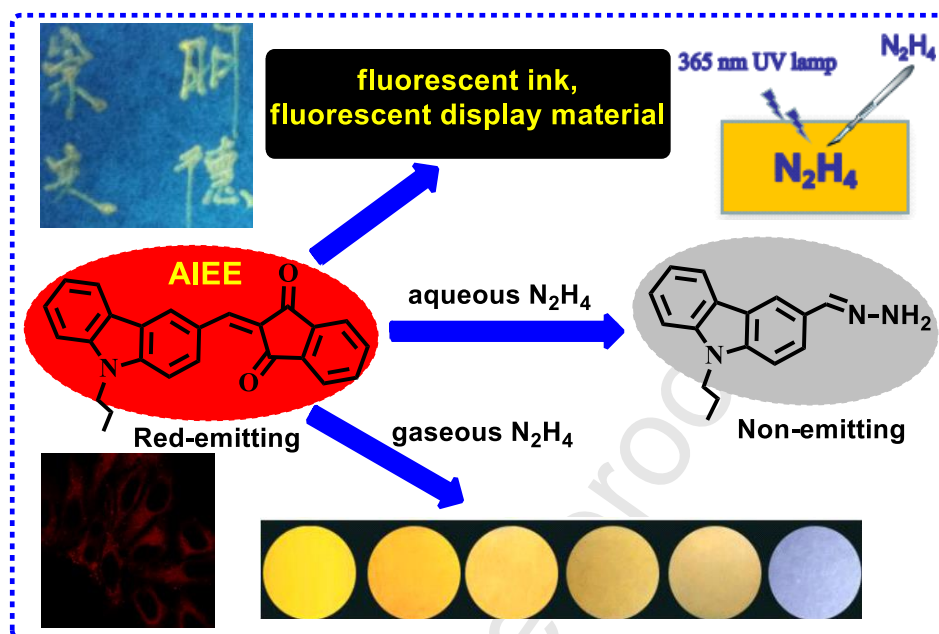
Xuyang Qin: Review & Editing.

Conflict of interest statement

The authors declared no conflicts of interest to this work.

Journal Pre-proof

Graphical Abstract



Highlights

- ◆ A new easy-to-prepare red-emitting sensor **CBI** was developed for hydrazine.
- ◆ **CBI** has good advantages of AIEE properties and large Stokes shift.
- ◆ **CBI** exhibits ultrafast response, high sensitivity and selectivity for N_2H_4 .
- ◆ **CBI** was applied for detection of hydrazine in solution, gas state, solid state and live cells.